



Absence of methamphetamine-induced conditioned place preference in *weaver* mutant mice

Yuiko Ikekubo^{1,2} | Soichiro Ide¹ | Yoko Hagino¹ | Kazutaka Ikeda^{1,2} 

¹Addictive Substance Project, Tokyo Metropolitan Institute of Medical Science, Tokyo, Japan

²Molecular and Cellular Medicine, Graduate School of Medical and Dental Sciences, Niigata University, Niigata, Japan

Correspondence

Kazutaka Ikeda, Addictive Substance Project, Tokyo Metropolitan Institute of Medical Science, 2-1-6 Kamikitazawa, Setagaya-ku, Tokyo 156-8506, Japan.
Email: ikeda-kz@igakuken.or.jp

Funding information

Japan Agency for Medical Research and Development, Grant/Award Number: JP18mk0101076, JP19dk0307071 and JP19ek0610011; Japan Society for the Promotion of Science, Grant/Award Number: 17K08612, 16H06276 and 16K15565; Smoking Research Foundation

Abstract

Aims: G protein-activated inwardly rectifying potassium (GIRK) channels are related to rewarding effects of addictive drugs. The GIRK2 subunit is thought to play key roles in the reward system. *Weaver* mutant mice exhibit abnormal GIRK2 function and different behaviors that are caused by several addictive substances compared with wild-type mice. However, mechanisms of reward-related alterations in *weaver* mutant mice remain unclear. The present study investigated changes in the rewarding effects of methamphetamine (METH) in *weaver* mutant mice.

Methods: The rewarding effects of METH (4.0 mg/kg) were investigated using the conditioned place preference (CPP) paradigm. Extracellular dopamine level in the nucleus accumbens (NAc) was measured by in vivo microdialysis. To identify brain regions that were associated with these changes in rewarding effects, METH-induced alterations of Fos expression were investigated by immunohistochemical analysis.

Results: *Weaver* mutant mice exhibited a significant decrease in METH-induced CPP and dopamine release in the NAc. Methamphetamine significantly increased Fos expression in the posterior NAc (pNAc) shell in wild-type but not in *weaver* mutant mice.

Conclusions: Methamphetamine did not induce rewarding effects in *weaver* mutant mice. The pNAc shell exhibited a significant difference in neuronal activity between wild-type and *weaver* mutant mice. The present results suggest that the absence of METH-induced CPP in *weaver* mutant mice is probably related to an innate reduction of dopamine and decreased neural activity in the pNAc shell that is partially attributable to the change of GIRK channel function. GIRK channels, especially those containing the GIRK2 subunit, appear to be involved in METH dependence.

KEYWORDS

CPP, GIRK, methamphetamine, reward, *weaver* mutant mice

1 | INTRODUCTION

The substance addiction such as drug, alcohol, and nicotine, and the behavioral addiction such as gambling and Internet are caused by

neurochemical changes within the brain.^{1,2} Although various brain regions and biomolecules have been reported to relate to the pathogenesis of addiction, it has not led to the development of effective addiction treatments. G protein-activated inwardly rectifying

This is an open access article under the terms of the Creative Commons Attribution-NonCommercial-NoDerivs License, which permits use and distribution in any medium, provided the original work is properly cited, the use is non-commercial and no modifications or adaptations are made.

© 2020 The Authors. *Neuropsychopharmacology Reports* published by John Wiley & Sons Australia, Ltd on behalf of The Japanese Society of Neuropsychopharmacology



potassium (GIRK) channels are reportedly related to acute rewarding effects or adaptations that occur with chronic exposure to various addictive drugs, such as opioids, γ -hydroxybutyrate (a designer club drug), cannabinoids, and alcohol.³ They are activated by ligand-stimulated $G_{i/o}$ -linked G protein-coupled receptors, which include opioid receptors, cannabinoid CB_1 receptors, serotonin 5-hydroxytryptamine-1A ($5HT_{1A}$) receptors, M2 muscarinic receptors, γ -aminobutyric acid-B ($GABA_B$) receptors, dopamine D_2 receptors, and adenosine A_1 receptors. In mammals, GIRK channels are expressed as four subunits (GIRK1-GIRK4). GIRK1, GIRK2, and GIRK3 subunits are distributed throughout the central nervous system, including in key regions that are involved in cognition, learning, memory, emotion, and motor function.⁴⁻⁷ The GIRK2 subunit plays a role in regulating addictive substance-induced behaviors. GIRK2 knockout mice exhibit alterations of behavioral effects of alcohol, including an increase in alcohol consumption, a decrease in alcohol dependence, the stimulation of motor activity, and a decrease in the anxiolytic action of alcohol.⁸ Moreover, cocaine-induced locomotor sensitization is enhanced in GIRK2 knockout mice, and intravenous cocaine self-administration is dramatically reduced.⁹

Weaver mutant mice have a spontaneously occurring autosomal recessive mutation of the *Girk2* gene that is mapped to chromosome 16. The single G-to-A transition in the *Girk2* gene replaces glycine with serine in the pore-forming region of the GIRK2 subunit.¹⁰ This *weaver* mutation leads to a reduction of GIRK2 function and causes abnormalities of dopamine signaling. Alcohol- and opioid-induced analgesia are reportedly reduced in *weaver* mutant mice.^{11,12} Furthermore, amphetamine caused less hyperlocomotion in *weaver* mutant mice, although direct dopamine receptor agonism, such as with apomorphine, increases motor activity.¹³ However, only few studies have investigated the rewarding effects of addictive substances in *weaver* mutant mice or the association between GIRK2 subunit functions and methamphetamine (METH) dependence. Therefore, the present study investigated changes in the rewarding effects of METH using *weaver* mutant mice.

2 | METHODS

2.1 | Animals

Heterozygous/heterozygous matings of *weaver* mutant mice on a C3H/HeJ Jcl background were used to produce wild-type, heterozygous, and homozygous *weaver* mutant mice. The mice were 16-20 weeks of age at the time of the experiments. The mice were housed 4-6 per cage in an environment at $23 \pm 1^\circ\text{C}$ and $50 \pm 5\%$ humidity with free access to food and water under a 12-h/12-h light/dark cycle.

2.2 | Drugs

Methamphetamine hydrochloride (Dainippon Sumitomo Pharma) was dissolved in saline and administered intraperitoneally (i.p.)

in a volume of 10 mL/kg body weight. All experiments were conducted with the METH dose at 4 mg/kg that reportedly induces not abnormal behaviors,¹⁴ but place preference in wild-type mice. Methamphetamine was freshly prepared for all of the experiments.

2.3 | Conditioned place preference test

The conditioned place preference (CPP) test was performed using a two-compartment Plexiglas chamber. One compartment (175 mm width \times 150 mm length \times 175 mm height) was black with a smooth floor. The other compartment had the same dimensions but was white with a textured floor. For the preconditioning, postconditioning, extinction, and priming phases, a T-style division with double 60 mm \times 60 mm openings allowed the mice to access both compartments. During the conditioning phases, the openings were eliminated to restrict the mice to one of the compartments. Locomotion and the time spent in each compartment were recorded using an animal activity monitoring apparatus that was equipped with an infrared detector (Neuroscience). The CPP apparatus was placed in a sound-attenuated, light-controlled box (~ 3100 lux). Conditioned place preference was assessed in five phases (preconditioning, conditioning, postconditioning, extinction, and priming). On days 1 and 2, the mice were allowed to freely explore both compartments through the openings for 900 seconds and acclimate to the apparatus. On day 3 (preconditioning phase), the same trial was performed, and the time spent in each compartment was measured for 900 seconds. We selected a counterbalanced protocol to nullify each mouse's initial preference as discussed previously.¹⁵ Biased mice that spent more than 80% of the time (ie, 720 seconds) on one side on day 3 or more than 600 seconds on one side on day 2 and more than 600 seconds on the other side on day 3 were excluded from further experiments. Conditioning was conducted once daily for 4 consecutive days (days 4-7). The mice were injected with either METH (4.0 mg/kg, i.p.) or saline and immediately confined to the black or white compartment for 50 minutes on day 4. On day 5, the mice were injected with alternate saline or METH injections and immediately confined to the opposite compartment for 50 minutes. On days 6 and 7, the same conditioning as on days 4 and 5 was repeated. The assignment of the mice to the conditioned compartment was performed randomly and counterbalanced across subjects. During the postconditioning phase on day 8, the time spent in each compartment was measured for 900 seconds without drug injection. After 28 days of the postconditioning phase (day 36), to confirm the extinction of CPP, the part of experimented mice was allowed to freely explore the two compartments through the openings for 900 seconds (extinction phase). The next day (day 37), 5 minutes after a low-dose METH priming injection (0.5 mg/kg, i.p.), the mice were free to explore the compartments for 900 seconds, and the time spent in each compartment was measured (priming phase). The CPP score and priming score were designated as the time spent in the drug-paired compartment on day 8 or day 37 minus the time spent in the same compartment in the preconditioning phase on day 3.



2.4 | Surgical implantation of microdialysis probes

The mice were stereotaxically implanted with microdialysis probes under sodium pentobarbital anesthesia (50 mg/kg, i.p.) in the nucleus accumbens (NAc; anterior, +0.8 to 1.54 mm; lateral, +1.0 mm; ventral, -5.0 mm from bregma) according to a mouse brain atlas.¹⁶ The probe tips were constructed with regenerated cellulose membranes that provided a 50 kDa molecular weight cutoff, 0.22 mm outer diameter, and 2 mm membrane length (Eicom). The dialysis probe placements were verified histologically at the end of the experiment. Data were excluded if the membrane portions of the dialysis probes were outside the NAc region.

2.5 | Microdialysis and analytical procedure

Twenty-four hours after implantation, the dialysis experiments were performed in freely moving mice. Ringer's solution (145 mmol/L Na⁺, 3 mmol/L K⁺, 1.26 mmol/L Ca²⁺, 1 mmol/L Mg²⁺, and 152.5 mmol/L Cl⁻, pH 6.5) was perfused at 1 μ L/min for 180 minutes. Baselines of extracellular dopamine concentrations were obtained from average concentrations of three consecutive samples when they were stable. Perfusates were directly injected into the high-performance liquid chromatography system every 10 minutes using an autoinjector (EAS-20; Eicom). Dialysate dopamine was separated using a PP-ODS reverse-phase column (Eicom) and ECD-100 graphite electrode detector (HTEC-500; Eicom). The mobile phase consisted of 0.1 mol/L phosphate buffer (pH 5.5) that contained sodium decanesulfonate (500 mg/L), ethylenediaminetetraacetic acid (50 mg/L), and 1% methanol. The dopamine detection limit was 0.3 fmol/sample, with a signal-to-noise ratio of at least 2.

2.6 | Fos immunohistochemistry

The mice were injected with either METH (4.0 mg/kg, i.p.) or saline and immediately confined to the black or white compartment of the CPP apparatus for 50 minutes. Two hours after the drug injection (reached peak Fos protein expression), the mice were deeply anesthetized with an overdose of sodium pentobarbital and transcardially perfused with 50 mL phosphate-buffered saline (PBS), followed by ice-cold 4% paraformaldehyde in 0.1 mol/L phosphate buffer (PB; pH 7.4). The brains were quickly removed from the skull and post-fixed overnight in the same fixative solution. After fixation, the brains were cryoprotected in 20% sucrose in 0.1 mol/L PB for 2 days at 4°C and serially sectioned (16 μ m thickness) using an HM550 cryostat (Thermo Fisher Scientific). The sections were blocked for 1 hour at room temperature in PBS that contained 0.3% Triton (PBST) with 5% bovine serum albumin (BSA), followed by incubation for 5 days at 4°C in c-Fos primary antibody (1:5000; catalog no. 226003, Synaptic Systems) in PBST with 5% BSA. After being washed with PBST three times, the sections were incubated with Alexa 647-conjugated donkey anti-rabbit IgG (1:1000; catalog no. ab150075, Abcam) in PBST

with 5% BSA for 1 hour at room temperature and then washed with PBST three times. The sections were then incubated with Hoechst 33342 (1:10 000; Thermo Fisher Scientific) in PBS for 5 minutes at room temperature for nuclear staining. Control and experimental tissues from each group were processed in parallel. No staining was observed in brain sections with omission of either the primary or secondary antibody.

2.7 | Cell counting

The number of Fos-positive nuclei was evaluated using fluorescence microscopy (BZ-X800; Keyence) at 20 \times magnification. Based on Fos expression and its relevance to drug dependence, the following brain regions were selected for counting Fos-immunoreactive cells: anterior NAc (aNAc) core, aNAc shell (1.34 mm from bregma), posterior NAc (pNAc) core, pNAc shell (0.98 mm from bregma), and ventral tegmental area (VTA; -3.16 mm from bregma) according to a mouse brain atlas.¹⁶ The analyses of the number of Fos-positive nuclei were performed using hybrid cell counts (BZ-X800 Analyzer; Keyence) to automatically count Fos-labeled cells in the region of interest. The measurement condition of the cell counter was set equally, and the number of Fos-positive nuclei was normalized to the area (mm²).

2.8 | Statistical analysis

All of the data were normally distributed and are expressed as the mean \pm the standard error of the mean (SEM). The data were analyzed using one-way analysis of variance (ANOVA) followed by Sidak's multiple-comparison *post hoc* test, Student's *t* test, or paired *t* test using Prism 7 software (GraphPad). Values of *P* < .05 were considered statistically significant.

3 | RESULTS

3.1 | Loss of rewarding effects of METH in weaver mutant mice

To assess the relationship between functional changes in GIRK2 and the rewarding effects of METH, we conducted the METH-induced CPP test in wild-type mice, heterozygous *weaver* mutant mice, and homozygous *weaver* mutant mice. Methamphetamine significantly increased the time spent in the previously drug-paired compartment in wild-type mice (preconditioning: 442.6 \pm 35.2 seconds; postconditioning: 562.2 \pm 27.8 seconds; *P* = .004, paired *t* test; Figure 1A). No significant difference was found between the preconditioning phase and extinction phase after 28 days of the postconditioning phase (preconditioning: 442.6 \pm 35.2 seconds; extinction: 504.2 \pm 31.4 seconds; *P* = .21, paired *t* test; Figure 1A). On the following day, a significant increase in the time spent in the previously drug-paired compartment was found in wild-type mice between

the priming phase and preconditioning phase (preconditioning: 442.6 ± 35.2 seconds; priming: 638.9 ± 35.4 seconds; $P < .001$, paired t test; Figure 1A). Heterozygous *weaver* mutant mice exhibited a trend toward an increase in the time spent in the drug-paired compartment in the postconditioning phase compared with the preconditioning phase (preconditioning: 454.3 ± 36.4 seconds; postconditioning: 539.7 ± 48.9 seconds; $P = .15$, paired t test; Figure 1A) and a significant increase in the priming phase compared with the preconditioning phase (preconditioning: 454.3 ± 36.4 seconds; priming: 560.5 ± 62.4 seconds; $P = .034$, paired t test; Figure 1A). No significant difference in METH-induced CPP was observed in any of the tests in homozygous *weaver* mutant mice (preconditioning: 455.7 ± 26.0 seconds; postconditioning: 416.6 ± 49.8 seconds;

priming: 484.5 ± 59.0 seconds; Figure 1A). The one-way ANOVA of CPP scores showed significant differences between homozygous *weaver* mutant mice and wild-type mice ($F_{2,30} = 3.81$, $P = .034$). *Post hoc* comparisons indicated that METH-induced CPP scores were significantly higher in wild-type mice than in homozygous *weaver* mutant mice ($P = .040$, Sidak's multiple-comparison *post hoc* test; Figure 1B). Similarly, the one-way ANOVA of priming scores indicated significant differences between homozygous *weaver* mutant mice and wild-type mice ($F_{2,26} = 3.58$, $P = .042$). The *post hoc* comparisons indicated a significant difference between homozygous *weaver* mutant mice and wild-type mice ($P = .041$, Sidak's multiple-comparison *post hoc* test; Figure 1C).

3.2 | Methamphetamine-induced increase in dopamine release in the NAc in *weaver* mutant mice decreased compared with wild-type mice

We next examined the effects of METH on dopamine release in the NAc in wild-type mice and homozygous *weaver* mutant mice using *in vivo* microdialysis. Baseline extracellular dopamine levels in the NAc were significantly different between wild-type and *weaver* mutant mice ($P = .018$, Student's t test). Mean baseline dopamine levels in the NAc were 0.187 ± 0.030 ng/10 μ L in wild-type mice ($n = 19$) and 0.091 ± 0.017 ng/10 μ L in homozygous *weaver* mutant mice ($n = 14$). Methamphetamine significantly increased dopamine release in the NAc in wild-type mice (one-way ANOVA: $F_{1,99,15,92} = 23.25$, $P < .001$; Figure 2A). Although *weaver* mutant mice exhibited a METH-induced increase in dopamine release, the extent of the increase was milder than in wild-type mice (one-way ANOVA, $F_{2,05,16,36} = 15.62$, $P < .001$; Figure 2A). The one-way ANOVA of the temporal course of the effects of METH on changes in dopamine release during a 180-minute interval after the injection, reflected by a cumulative response (ie, area under the curve [AUC]), showed significant differences in dopamine release in the NAc between groups ($F_{3,29} = 24.94$, $P < .001$). The *post hoc* comparisons indicated that METH significantly increased dopamine release in both homozygous *weaver* mutant mice and wild-type mice compared with saline treatment (wild-type mice, $P < .001$; homozygous *weaver* mutant mice, $P = .002$, Sidak's multiple-comparison *post hoc* test). The extent of the increase in dopamine levels in METH-treated homozygous *weaver* mutant mice was significantly lower than in METH-treated wild-type mice ($P = .047$, Sidak's multiple-comparison *post hoc* test; Figure 2B).

3.3 | Methamphetamine-induced Fos expression in the pNAc shell was suppressed in *weaver* mutant mice

To evaluate the possible relationship between neuronal activation and our *in vivo* results, we analyzed Fos expression in the aNAc core, aNAc shell, pNAc core, pNAc shell, and VTA using immunohistochemistry. Representative photomicrographs of Fos-positive nuclei

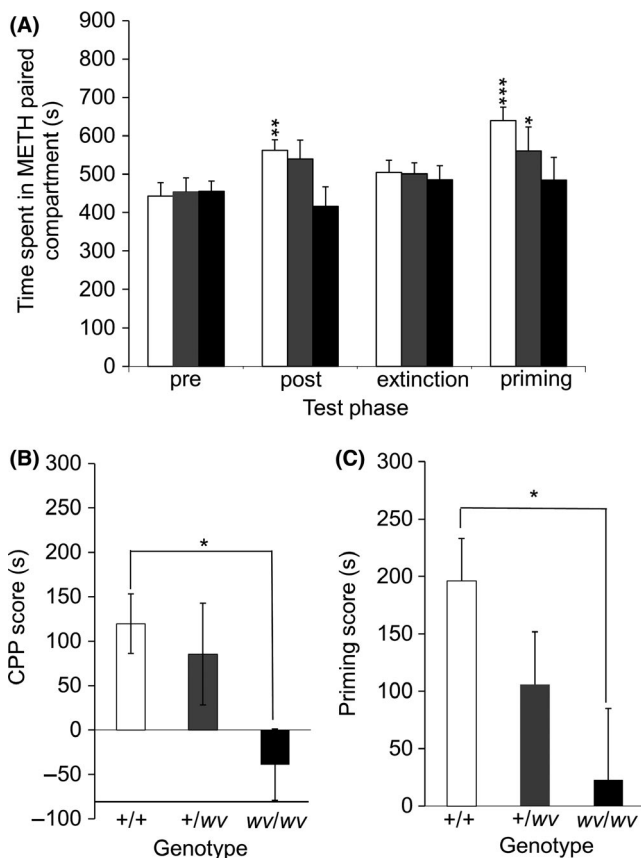


FIGURE 1 Rewarding and priming effects of METH in wild-type mice, heterozygous *weaver* mutant mice, and homozygous *weaver* mutant mice. A, Time spent in the METH-paired compartment in wild-type mice (+/+), heterozygous *weaver* mutant mice (+/-), and homozygous *weaver* mutant mice (-/-) in the preconditioning (pre), postconditioning (post), extinction (extinction), and priming (priming) phases. The columns and vertical lines represent the mean \pm SEM. * $P < .05$, ** $P < .01$, *** $P < .001$, compared with preconditioning phase in each genotype of mice. B, Conditioned place preference scores in each genotype of mice (+/+, $n = 11$; +/-, $n = 11$; -/-, $n = 11$). C, Priming scores in each genotype of mice (+/+, $n = 11$; +/-, $n = 11$; -/-, $n = 7$). The columns and vertical lines represent the mean \pm SEM. * $P < .05$, compared with wild-type mice

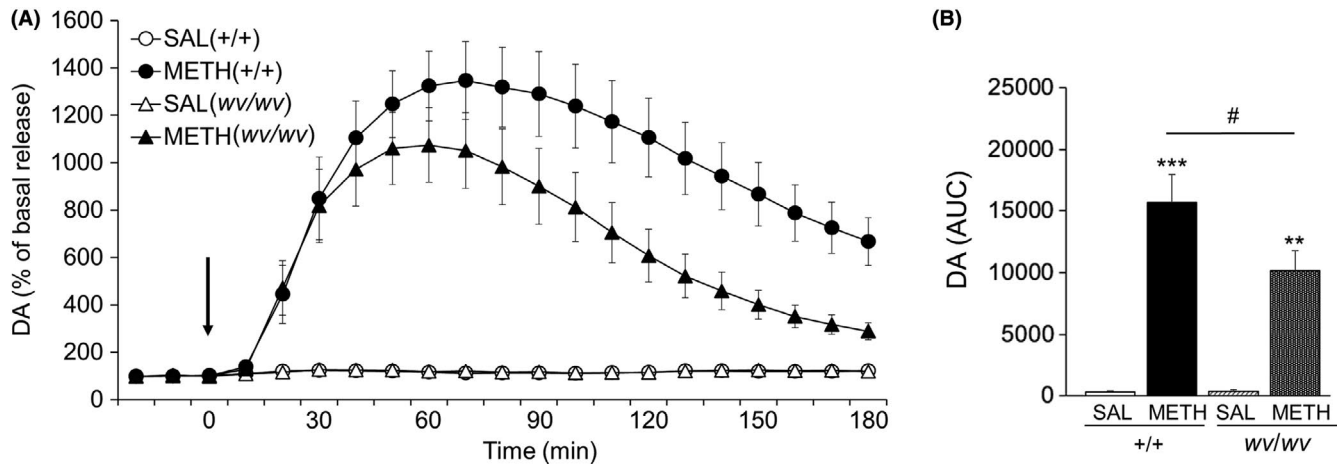


FIGURE 2 Changes in extracellular dopamine (DA) levels in the NAC in wild-type and *weaver* mutant mice that received saline (SAL) or METH. A, Temporal pattern of extracellular DA levels (+/+–SAL, $n = 10$; +/+–METH, $n = 9$; wv/wv–SAL, $n = 5$; wv/wv–METH, $n = 9$). The arrow indicates the time point of injection. The marks and vertical lines represent the mean \pm SEM of the percentage of control baselines. B, The mean AUC of extracellular DA levels in NAC during the 180-min interval after the injection (+/+–SAL, $n = 10$; +/+–METH, $n = 9$; wv/wv–SAL, $n = 5$; wv/wv–METH, $n = 9$). The columns and vertical lines represent the mean \pm SEM. ** $P < .01$, *** $P < .001$, compared with saline treatment for the same genotype; # $P < .05$, compared with wild-type mice

in the pNAC shell in wild-type and homozygous *weaver* mutant mice after saline or METH (4.0 mg/kg, i.p.) administration are shown in Figure 3A. The two-way ANOVA indicated a significant difference in the number of Fos-positive nuclei in the pNAC shell (drug \times genotype interaction, $F_{1,16} = 65.54$, $P < .001$; main effect of drug, $F_{1,16} = 54.10$, $P < .001$; main effect of genotype, $F_{1,16} = 32.90$, $P < .001$) and VTA (drug \times genotype interaction, $F_{1,16} = 3.14$, $P = .096$; main effect of drug, $F_{1,16} = 5.98$, $P = .026$; main effect of genotype, $F_{1,16} = 2.43$, $P = .14$), but no differences were found in the other brain regions (Figure 3B–F). In the pNAC shell, the *post hoc* comparisons indicated that METH significantly increased the number of Fos-positive nuclei in wild-type mice ($P < .001$, Sidak's multiple-comparison *post hoc* test). Methamphetamine-induced Fos expression was significantly lower in homozygous *weaver* mutant mice compared with METH-treated wild-type mice ($P < .001$, Sidak's multiple-comparison *post hoc* test). No differences were found in the other brain regions between the METH-treated and saline-treated groups.

4 | DISCUSSION

We investigated changes in the rewarding effects of METH in *weaver* mutant mice in the CPP test. Methamphetamine induced both CPP and priming effects in wild-type mice but not in *weaver* mutant mice. Although METH-induced CPP and priming effects increased in heterozygous *weaver* mutant mice, they were decreased compared with wild-type mice. *Weaver* mutant mice are known to exhibit ataxia, characterized by mild locomotor hyperactivity.¹³ Thus, the abolishment of METH-induced rewarding effects in the present study does not appear to be attributable to abnormal gait-related locomotor activity. The present results suggest that decreases in METH-induced CPP and priming effects are attributable to the copy number of the *weaver* mutant gene.

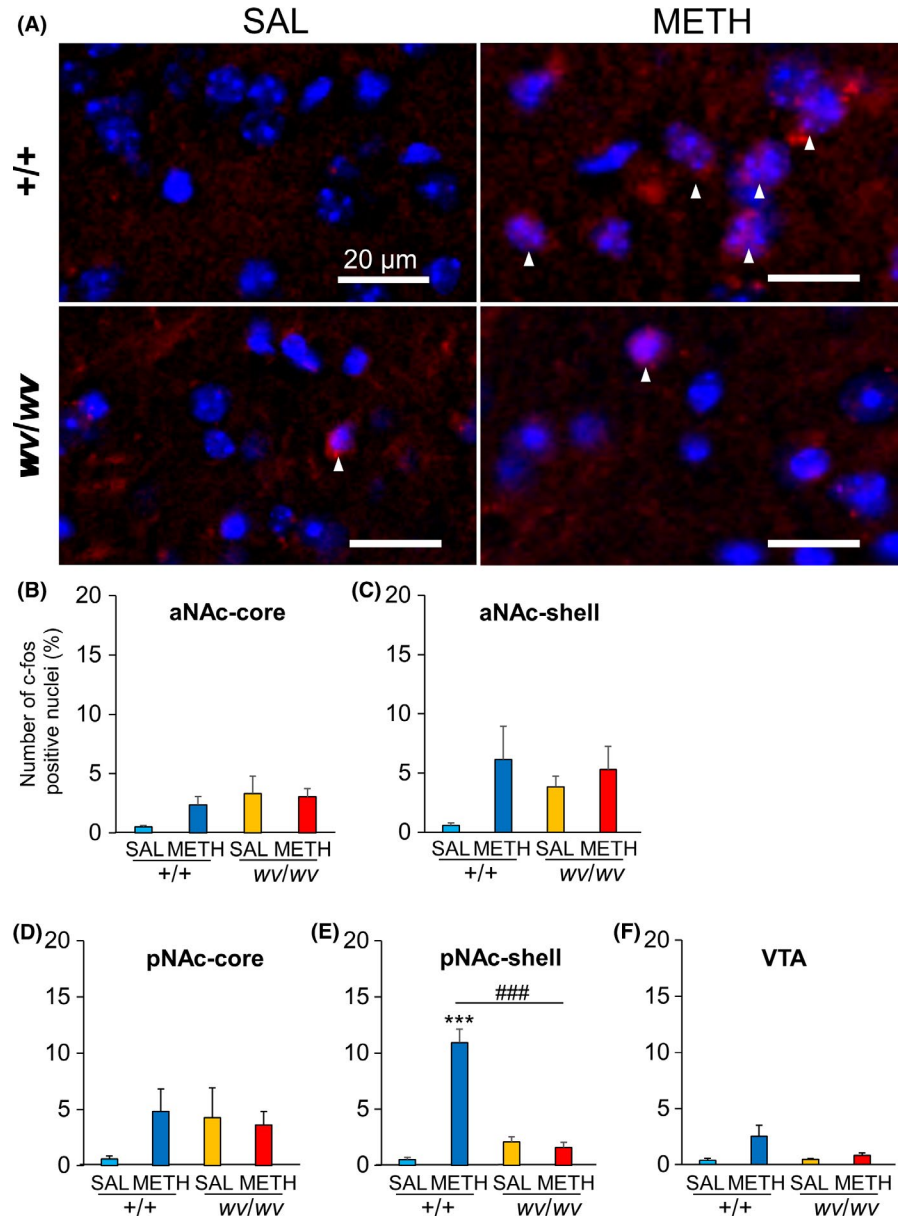
Based on these results, we measured changes in dopamine release in the NAC after METH administration in wild-type and homozygous *weaver* mutant mice. The baseline release of dopamine in *weaver* mutant mice was lower than in wild-type mice. Although METH increased dopamine release in both *weaver* mutant mice and wild-type mice, the extent of the increase in *weaver* mutant mice was milder than in wild-type mice. Several studies have reported that the rewarding effects of addictive substances are associated with dopamine release in the NAC.¹⁷ Thus, the disappearance of METH-induced CPP in *weaver* mutant mice may be at least partially attributable to alterations of dopamine signaling in the NAC.

Supporting the *in vivo* results, we conducted immunohistochemical analyses to reveal brain regions where neuronal activation by METH was altered in *weaver* mutant mice. We analyzed alterations of Fos protein expression, a well-known marker of neuronal activation, in five brain regions that are related to the reward system: aNAC core, aNAC shell, pNAC core, pNAC shell, and VTA. Methamphetamine treatment increased the number of Fos-positive nuclei in the pNAC shell in wild-type mice. In *weaver* mutant mice, no difference in Fos expression was found between saline and METH treatment in any of the brain regions. These results suggest that the pNAC shell plays an important role in the absence of METH-induced CPP in *weaver* mutant mice. The absence of METH-induced CPP in *weaver* mutant mice may have several explanations as discussed below.

4.1 | Influence of dopamine reduction in *weaver* mutant mice on METH-induced CPP

Dopamine depletion was observed in the brain in *weaver* mutant mice. In the NAC, dopamine levels decreased by 43% in heterozygous *weaver* mutant mice and by 24% in homozygous *weaver* mutant mice

FIGURE 3 Methamphetamine-induced changes in Fos expression in various brain regions in wild-type and *weaver* mutant mice. A, Photomicrographs illustrate the immunohistochemical labeling of Hoechst 33342 (blue) and Fos (red) in coronal sections of the pNAc shell (left upper panel, saline-treated wild-type mice; right upper panel, METH-treated wild-type mice; left lower panel, saline-treated *weaver* mutant mice; right lower panel, METH-treated *weaver* mutant mice). Arrowheads point to the colocalization of Fos staining and nuclear staining. B-F, Quantification of the number of Fos-positive nuclei in saline- and METH-treated *weaver* mutant mice in the aNAc core, aNAc shell, pNAc core, pNAc shell, and VTA (+/+–SAL, $n = 5$; +/+–METH, $n = 5$; *wv/wv*–SAL, $n = 5$; *wv/wv*–METH, $n = 5$). The columns and vertical lines represent the mean \pm SEM. *** $P < .001$, compared with saline treatment for the same genotype; ### $P < .001$, compared with wild-type mice for the same treatment



compared with wild-type mice.¹⁸ The expression of both dopamine D₁ receptors and dopamine D₂ receptors was previously reported to not be different between wild-type and *weaver* mutant mice.¹⁸ In the present study, we found that baseline extracellular dopamine levels were lower in *weaver* mutant mice than in wild-type mice. The METH-induced increase in dopamine levels was less in *weaver* mutant mice than in wild-type mice. These results, together with previous reports, suggest that total levels of dopamine or changes in dopamine release in the NAc may be involved in the abolishment of METH-induced CPP in *weaver* mutant mice.

4.2 | Influence of abnormal GIRK2 subunit activation on METH-induced CPP

The activation of GIRK channels plays an important role in various brain functions, such as pain perception, analgesia, rewarding

effects, and memory modulation. Ifenprodil, which inhibits the function of not only *N*-methyl-D-aspartate receptors but also GIRK channels,¹⁹ suppressed morphine-induced CPP.²⁰ Additionally, paroxetine and fluoxetine but not fluvoxamine inhibited METH-induced CPP. Although these drugs are selective serotonin reuptake inhibitors, paroxetine and fluoxetine but not fluvoxamine inhibit GIRK channels. Thus, the inhibition of GIRK channels may be partially involved in the inhibition of METH-induced CPP.²¹ Furthermore, the METH- and cocaine-induced dysfunction of inhibitory GABA_B-GIRK signaling in VTA GABAergic neurons²² were shown to enhance excitatory VTA dopaminergic neurons, resulting in an increase in dopamine release in the NAc and medial prefrontal cortex. These previous findings suggest that the absence of METH-induced CPP in *weaver* mutant mice in the present study may have been caused by alterations of neurotransmission in the reward system that resulted from impairments in GIRK channel function.



4.3 | Attenuation of reward-related learning and memory

The NAc plays an important role in reward processing. Reward-related information, such as reward seeking and reward consumption, is integrated by the NAc in cooperation with various brain regions, such as the hippocampus (HPC; memory), basolateral amygdala (drive and motivation), VTA (reward prediction), and ventral pallidum (goal-directed motor response).²³ Anatomical studies have demonstrated that the NAc is divided into two functionally distinct areas, the core and shell. The NAc shell and HPC pathway are related to reward- or drug-seeking behavior, followed by spatial and contextual conditioning information. The NAc core and dopaminergic circuit are related to reward- and drug-seeking behavior that is elicited by discrete cues that are associated with reward-related substances.²⁴ The CPP procedure is a widely used model that reveals associations between rewarding effects of drugs and environmental information, such as visual and olfactory cues. Spatial or contextual memory consolidation is very important in the acquisition of CPP. Nicotine-induced CPP was decreased by dopamine ablation in the NAc shell, whereas nicotine-induced CPP was enhanced by dopamine ablation in the NAc core.²⁵ Similarly, the repeated amphetamine administration-induced increase in dopamine levels in the NAc shell enhances spatial conditioning, but this increase attenuates cue conditioning during the acquisition of CPP. These studies indicate that hyperactivity of the dopamine system from the NAc shell to HPC facilitates signal transduction during new associative learning.²⁶ In the present study, METH-induced neuronal activation was observed in the NAc shell in wild-type mice. These results, together with previous studies, suggest that the METH-induced increase in Fos-positive nuclei in the NAc shell represents a hyperdopaminergic state that is involved in reward-related learning and memory consolidation in the CPP paradigm. In contrast, *weaver* mutant mice, which did not exhibit METH-induced CPP, exhibited a decrease in Fos expression in the NAc shell compared with METH-treated wild-type mice. GIRK-regulated signaling also plays an important role in learning and memory processes. Several studies reported GIRK-mediated currents in brain regions that are related to spatial and contextual learning, cognitive function, and the establishment of reward-related memory. Furthermore, dopamine signaling in the VTA is involved in the association between learning and addiction. The activity of GIRK channels is also partially involved in this process.⁷ Based on the present results and previous findings, *weaver* mutant mice may exhibit impairments in reward-related learning and memory processes that are attributable to abnormal GIRK2 subunit function. Consequently, the absence of METH-induced CPP in *weaver* mutant mice might result from a failure to remember the drug-paired compartment. However, although CPP can be tested in *weaver* mutant mice, other forms of cognition (eg, learning and memory) are impossible to test in *weaver* mutant mice because of their gross motor impairments. Thus, proving the above hypothesis based solely on the present results is difficult.

In the present study, we observed the absence of METH-induced CPP and a METH-induced decrease in extracellular dopamine release

in *weaver* mutant mice. We also found significant differences in neuronal activity, reflected by Fos expression, in the pNAc shell after METH treatment between wild-type mice and *weaver* mutant mice. Our results suggest that defective neuronal activity in the pNAc shell that occurs through a direct or indirect influence of abnormal GIRK2 subunit function is involved in the absence of METH-induced CPP in *weaver* mutant mice.

G protein-activated inwardly rectifying potassium channels are key factors in the development and maintenance of drug dependence. Our group previously reported that the GIRK channel inhibitor ifenprodil inhibited alcohol use in patients with alcohol dependence.²⁷ Although medications exist for the treatment of opioid and alcohol dependence, no effective pharmacological treatments have been discovered for psychostimulant dependence. Our group is currently conducting a clinical trial to examine the effects of ifenprodil in patients with METH dependence.²⁸ Further animal and clinical studies will determine whether GIRK inhibitors are effective for the treatment of addiction.

ACKNOWLEDGMENTS

The authors are grateful to M. Arends for English editing and also thank E. Kamegaya and Y. Matsushima for technical assistance. This work was supported by JSPS KAKENHI (no. 16K15565 and 16H06276 to KI; no. 17K08612 to SI), AMED (no. JP19dk0307071, JP18mk0101076, and JP19ek0610011 to KI), and the Smoking Research Foundation (KI).

CONFLICT OF INTEREST

The authors declare no conflicts of interest for this article.

AUTHOR CONTRIBUTION

YI, SI, and KI were involved in the conception and design of the experiments. YI, SI, and YH performed the experiments and statistical analyses and wrote the manuscript. YI, SI, and KI finalized the manuscript. All of the authors read and approved the final manuscript.

ETHICAL APPROVAL

The experimental procedures and housing conditions were approved by the Institutional Animal Care and Use Committee (permission number: 20-019), and all of the animals were cared for and treated humanely in accordance with our institutional animal experimentation guidelines.

DATA AVAILABILITY STATEMENT

The data that support the findings of this study are available in the supplementary material of this article.

ORCID

Kazutaka Ikeda  <https://orcid.org/0000-0001-8342-0278>

REFERENCES

1. Kuhn BN, Kalivas PW, Bobadilla AC. Understanding addiction using animal models. *Front Behav Neurosci.* 2019;13:262.

2. Ford M, Hakansson A. Problem gambling, associations with comorbid health conditions, substance use, and behavioural addictions: Opportunities for pathways to treatment. *PLoS One*. 2020;15(1):e0227644.
3. Luscher C, Slesinger PA. Emerging roles for G protein-gated inwardly rectifying potassium (GIRK) channels in health and disease. *Nat Rev Neurosci*. 2010;11(5):301–15.
4. Ikeda K, Kobayashi T, Kumanishi T, Yano R, Sora I, Niki H. Molecular mechanisms of analgesia induced by opioids and ethanol: is the GIRK channel one of the keys? *Neurosci Res*. 2002;44(2):121–31.
5. Rifkin RA, Moss SJ, Slesinger PA. G protein-gated potassium channels: a link to drug addiction. *Trends Pharmacol Sci*. 2017;38(4):378–92.
6. Lesage F, Guillemare E, Fink M, et al. Molecular properties of neuronal G-protein-activated inwardly rectifying K⁺ channels. *J Biol Chem*. 1995;270(48):28660–7.
7. Tipps ME, Buck KJ. GIRK channels: a potential link between learning and addiction. *Int Rev Neurobiol*. 2015;123:239–77.
8. Blednov YA, Stoffel M, Chang SR, Harris RA. Potassium channels as targets for ethanol: studies of G-protein-coupled inwardly rectifying potassium channel 2 (GIRK2) null mutant mice. *J Pharmacol Exp Ther*. 2001;298(2):521–30.
9. Morgan AD, Carroll ME, Loth AK, Stoffel M, Wickman K. Decreased cocaine self-administration in Kir3 potassium channel subunit knockout mice. *Neuropsychopharmacology*. 2003;28(5):932–8.
10. Patil N, Cox DR, Bhat D, Faham M, Myers RM, Peterson AS. A potassium channel mutation in weaver mice implicates membrane excitability in granule cell differentiation. *Nat Genet*. 1995;11(2):126–9.
11. Kobayashi T, Ikeda K, Kojima H, et al. Ethanol opens G-protein-activated inwardly rectifying K⁺ channels. *Nat Neurosci*. 1999;2(12):1091–7.
12. Ikeda K, Kobayashi T, Kumanishi T, Niki H, Yano R. Involvement of G-protein-activated inwardly rectifying K (GIRK) channels in opioid-induced analgesia. *Neurosci Res*. 2000;38(1):113–6.
13. Schmidt MJ, Sawyer BD, Perry KW, Fuller RW, Foreman MM, Ghetti B. Dopamine deficiency in the weaver mutant mouse. *J Neurosci*. 1982;2(3):376–80.
14. Yamanaka Y, Takano R, Egashira T. Methamphetamine-induced behavioral alterations following repeated administration of methamphetamine. *Jpn J Pharmacol*. 1986;41(2):147–54.
15. Tzschentke TM. Measuring reward with the conditioned place preference paradigm: a comprehensive review of drug effects, recent progress and new issues. *Prog Neurobiol*. 1998;56(6):613–72.
16. Paxinos G, Franklin KBJ. The mouse brain in stereotaxic coordinates, 2nd edn. San Diego, CA: Academic Press; 2001.
17. Luscher C, Malenka RC. Drug-evoked synaptic plasticity in addiction: from molecular changes to circuit remodeling. *Neuron*. 2011;69(4):650–63.
18. Reader TA, Ase AR, Hebert C, Amdiss F. Distribution of dopamine, its metabolites, and D1 and D2 receptors in heterozygous and homozygous weaver mutant mice. *Neurochem Res*. 1999;24(11):1455–70.
19. Kobayashi T, Washiyama K, Ikeda K. Inhibition of G protein-activated inwardly rectifying K⁺ channels by ifenprodil. *Neuropsychopharmacology*. 2006;31(3):516–24.
20. Suzuki T, Kato H, Tsuda M, Suzuki H, Misawa M. Effects of the non-competitive NMDA receptor antagonist ifenprodil on the morphine-induced place preference in mice. *Life Sci*. 1999;64(12):PL151–6.
21. Takamatsu Y, Yamamoto H, Hagino Y, Markou A, Ikeda K. The selective serotonin reuptake inhibitor paroxetine, but not fluvoxamine, decreases methamphetamine conditioned place preference in mice. *Curr Neuropharmacol*. 2011;9(1):68–72.
22. Padgett CL, Lalive AL, Tan KR, et al. Methamphetamine-evoked depression of GABA(B) receptor signaling in GABA neurons of the VTA. *Neuron*. 2012;73(5):978–89.
23. Day JJ, Roitman MF, Wightman RM, Carelli RM. Associative learning mediates dynamic shifts in dopamine signaling in the nucleus accumbens. *Nat Neurosci*. 2007;10(8):1020–8.
24. Ito R, Robbins TW, Pennartz CM, Everitt BJ. Functional interaction between the hippocampus and nucleus accumbens shell is necessary for the acquisition of appetitive spatial context conditioning. *J Neurosci*. 2008;28(27):6950–9.
25. Sellings LH, Baharnouri G, McQuade LE, Clarke PB. Rewarding and aversive effects of nicotine are segregated within the nucleus accumbens. *Eur J Neurosci*. 2008;28(2):342–52.
26. Ito R, Hayden A. Opposing roles of nucleus accumbens core and shell dopamine in the modulation of limbic information processing. *J Neurosci*. 2011;31(16):6001–7.
27. Sugaya N, Ogai Y, Aikawa Y, et al. A randomized controlled study of the effect of ifenprodil on alcohol use in patients with alcohol dependence. *Neuropsychopharmacol Rep*. 2018;38(1):9–17.
28. Kotajima-Murakami H, Takano A, Ogai Y, et al. Study of effects of ifenprodil in patients with methamphetamine dependence: protocol for an exploratory, randomized, double-blind, placebo-controlled trial. *Neuropsychopharmacol Rep*. 2019;39(2):90–9.

SUPPORTING INFORMATION

Additional supporting information may be found online in the Supporting Information section.

How to cite this article: Ikekubo Y, Ide S, Hagino Y, Ikeda K. Absence of methamphetamine-induced conditioned place preference in weaver mutant mice. *Neuropsychopharmacol Rep*. 2020;40:324–331. <https://doi.org/10.1002/npr2.12130>